

Binuclear Copper(II) Oxidation Products from Copper(I) Complexes with Tridentate Ligands. Magnetostructural Characterization

Darío Rojas, Ana M. García, Andrés Vega,[†] Yanko Moreno,[‡] Diego Venegas-Yazigi, María T. Garland, and Jorge Manzur**Departamento de Química, Facultad de Ciencias Físicas y Matemáticas, Universidad de Chile, Tupper 2069, Santiago, Chile*

Received March 16, 2004

The bis-pyridine tridentate ligands (6-R-2-pyridylmethyl)–(2-pyridylmethyl) benzylamine (RDPMA, where R = CH₃, CF₃), (6-R-2-pyridylmethyl)–(2-pyridylethyl) benzylamine (RPMPEA, where R = CH₃, CF₃), and the bidentate ligand di-benzyl-(6-methyl-2-pyridylmethyl)amine (BiBzMePMA) have been synthesized and their copper(I) complexes oxidized in a methanol solution to afford self-assembled bis- μ -methoxy-binuclear copper(II) complexes (**1**, **2**, **4**, **6**) or hydroxo- binuclear copper(II) complexes (**3**). Oxidation of the nonsubstituted DPMA (R = H) in dichloromethane gives a chloride-bridged complex (**5**). The crystal structures for [Cu(MeDPMA)(MeO)]₂(ClO₄)₂ (**1**), [Cu(RPMPEA)(MeO)]₂(ClO₄)₂ (for **2**, R = Me, and for **4**, R = CF₃), [Cu(BiBzMePMA)(MeO)]₂(ClO₄)₂ (**6**), [Cu(FDPMA)(OH)]₂(ClO₄)₂ (**3**), and [Cu(DPMA)(Cl)]₂(ClO₄)₂ (**5**) have been determined, and their variable-temperature magnetic susceptibility has been measured in the temperature range of 10–300 K. The copper coordination geometries are best described as square pyramidal, except for **6**, which is square planar, because of the lack of one pyridine ring in the bidentate ligand. In **1–4** and **6**, the basal plane is formed by two pyridine N atoms and two O atoms from the bridging methoxy or hydroxo groups, whereas in **5**, the bridging Cl atoms occupy axial–equatorial sites. Magnetic susceptibility measurements show that the Cu atoms are strongly coupled antiferromagnetically in the bis-methoxy complexes **1**, **2**, **4**, and **6**, with $-2J > 600 \text{ cm}^{-1}$, whereas for the hydroxo complex **3**, $-2J = 195 \text{ cm}^{-1}$ and the chloride-bridged complex **5** shows a weak ferromagnetic coupling, with $2J = 21 \text{ cm}^{-1}$ ($2J$ is an indicator of the magnetic interaction between the Cu centers).

Introduction

The coordination chemistry of copper complexes is a subject of continuing importance, in relation to the structures and reactivity of the active sites in copper-containing metalloproteins. The reactivity of copper(I) complexes toward dioxygen is relevant to the utilization of atmospheric oxygen in stoichiometric or catalytic oxidations of organic substrates mediated by copper complexes,¹ as well as to the understanding of dioxygen utilization by copper proteins.^{1–3}

The structure and reactivity of copper complexes are altered significantly by subtle perturbations in the supporting ligands. Recent advances^{4,5} have shown that the ligand, i.e., its denticity, chelate ring size, donor type, substituents on or near N-donors, strongly influences copper–dioxygen chemistry. One remarkable example is the copper(I) complex of tris(2-pyridylmethyl)amine (TPMA), which afforded a (μ -1,2-peroxo) dicopper(II) complex in the reaction with oxygen at a low temperature ($-80 \text{ }^\circ\text{C}$),⁶ whereas the bis-methyl-substituted derivative bis(6-methyl-2-pyridylmethyl)(2-pyridylmethyl)amine (Me₂TPMA) produced a bis(μ -oxo)-dicopper(III) complex, under the same experimental conditions.⁷

The effects of the alkyl linker chain in these type of ligands have also been investigated to demonstrate that the longer

* Author to whom correspondence should be addressed. E-mail: jmanzur@dqb.uchile.cl.

[†] Present address: Universidad de Tarapacá.

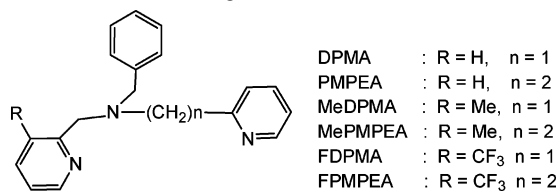
[‡] Present address: Universidad de Concepción.

- (1) Karlin, K. D.; Zuberbühler, A. D. In *Bioinorganic Catalysis*, Second Edition, Revised and Expanded; Reedik, J., Bouwman, E., Eds.; Marcel Dekker: New York, 1999; pp 469–534.
- (2) Kopf, M. A.; Karlin, K. D. In *Biomimetic Oxidations*; Meunier, B., Ed.; Imperial College Press: London, 2000; Chapter 7, pp 309–362.
- (3) Solomon, E. I.; Sundaram, U. M.; Machonkin, T. E. *Chem. Rev.* **1996**, *96*, 2563–2605.

(4) Kitajima, N.; Moro-oka, Y. *Chem. Rev.* **1994**, *94*, 737–757.

(5) Suzuki, M.; Furutachi, H.; Otawa, H. *Coord. Chem. Rev.* **2000**, *200–202*, 105–129.

Chart 1. New Tridentate Ligands



ethylene linker in bis(2-pyridylethyl)amine (TEPA) can adapt its copper(I) complex to a tetrahedral geometry, resulting unreactive toward dioxygen,⁸ in sharp contrast to the high reactivity of the TMPA analogue, whose geometry is described as trigonal bipyramidal.⁹

Mononucleating tridentate and dinucleating bis-tridentate ligands were also used to study the copper–oxygen chemistry. Usually, tetradentate N-donor ligands yield the end-on μ -1,2-peroxo coordination,^{4,5,8,10} whereas tridentate or bidentate N-donor ligands yield side-on μ - η^2 - η^2 -peroxo-dicopper(II) complexes, or related bis- μ -oxo-dicopper(III) species.^{4,5,11–14} It has been shown that these peroxo-oxo species normally are in rapid equilibrium.

Replacing all the C–H bonds of a methyl substituent of the ligand by C–F bonds resulted in a dramatic effect on the thermal stability of the copper–oxygen adduct. The copper(I) complex with the fluorinated ligand 3-trifluoromethyl-5-methyl-1-pyrazolyl borate (Tp^{CF₃,CH₃}) affords a binuclear μ - η^2 - η^2 -peroxo-dicopper(II) complex that is stable for days in a diluted solution at room temperature and is indefinitely stable at 25 °C as a purple solid. The protonated analogue Tp^{CH₃,CH₃} with similar copper–ligand topology forms a peroxo complex that is stable only at low temperature.¹³

In this work, we report on the syntheses of a series of tridentate ligands of the bis-pyridylamine type (Chart 1), in which the alkyl linker chain changes from methylene to ethylene and has a methyl or trifluoromethyl substituent at the 2-position of the pyridine ring, and the characterization of the copper(II) complexes resulting from the oxygenation of solutions of the corresponding copper(I) complexes in methanol at room temperature. We also prepared the bidentate ligand di-benzyl-(6-methyl-2-pyridylmethyl)amine (Bi-BzMePMA) and the corresponding copper(II) oxidation product. Attempts to detect and characterize copper–oxygen adducts at low temperature failed. The only products that

were isolated and characterized were the di-methoxy- or di-hydroxy-dicopper(II) complexes.

Experimental Section

The reagents and solvents used were of commercially available reagent quality, unless otherwise stated.

Measurements. Elemental analyses (C, H, and N) were performed at the CEPEDEQ (Center for the Chemistry Development of the University of Chile). The copper content was determined using atomic absorption spectroscopy (AAS). ¹H NMR spectra were recorded in CDCl₃ on a Bruker AMX-300 NMR spectrometer. Chemical shifts are reported as δ values downfield of an internal Me₄Si reference. Magnetic measurements in the 10–300 K temperature range were obtained on Cryogenic SQUID equipment. The experimental data were corrected for diamagnetism, using Pascal constants and temperature-independent paramagnetism ($N\alpha$); a value of 60×10^{-6} emu/mol per Cu atom was applied.

X-ray Crystallographic Data Collection and Refinement of the Structures. A single crystal was mounted on a glass fiber. The intensity data collection was made on a Bruker Smart Apex diffractometer, using separations of 0.3° between frames and 10 s by frame. Data integration was made using SAINT.¹⁵ The structures were solved using XS in SHELXTL,¹⁶ by means of direct methods and completed (non-H atoms) by Fourier difference synthesis. Refinement until convergence was obtained using XL SHELXTL¹⁶ and SHELXL97.¹⁶ Additional crystallographic and refinement details are given in Table 1.

Preparations. Di-2-pyridylmethylamine. Excess 2-pyridylmethylamine (0.1 mol) was reacted with 2-chloromethyl-pyridine (0.05 mol) in acetonitrile (200 mL) for 24 h, under reflux, with excess solid Na₂CO₃. The mixture was filtered and the solvent removed by distillation at reduced pressure. The residue was fractionally distilled to give the secondary amine (6.5 g, 65%, based on the chloride).

(2-Pyridylmethyl)(2-pyridylethyl)amine. This amine was obtained by the same method, using 2-pyridylethylamine (yield: 72%).

(2-Bromomethyl)(6-methyl)pyridine. Excess 2,6-dimethylpyridine (1 mol) was added to a suspension of *N*-bromo-succinimide (NBS) (0.38 mol) in 200 cm³ of dried CCl₄. The reaction mixture was refluxed with stirring for 2 h, under UV light. After this time, the red solution was allowed to cool and the precipitate was filtered off and washed three times with CCl₄. The resultant combined solution was concentrated in vacuo and distilled to yield a reddish oil product that solidified on cooling (yield: 25%).

(2-Trifluoromethyl)(6-methyl)pyridine. This compound was obtained by reaction of (6-methyl)-2-picolinic acid¹⁷ with SF₄ in liquid HF at 120 °C under pressure in an autoclave. Twenty grams of (6-methyl)-2-picolinic acid and 23 g of liquid HF were added into a stainless-steel reactor with a capacity of 250 cm³. With the aid of a vacuum line, 40 g of SF₄ gas was transferred to the reactor through the reactor inlet and then the inlet valve was closed. The reactor was heated in an oil bath at 120 °C for 18 h and then allowed to cool at room temperature; the excess SF₄ and the SOF₂ byproduct were eliminated carefully to a cooled trap. The reaction mixture was diluted with 60 cm³ of cooled water, made alkaline with 8 M NaOH and steam distilled. The obtained oil was separated, the aqueous phase was washed three times with 25 cm³

- (6) Jacobson, R. R.; Tyeklar, Z.; Farooq, A.; Karlin, K. D.; Liu, S.; Zubieta, J. *J. Am. Chem. Soc.* **1988**, *110*, 3690–3692.
 (7) Hayashi, H.; Fujimani, S.; Nagatomo, S.; Ogo, S.; Suzuki, M.; Uehara, A.; Watanabe, Y.; Kitagawa, T. *J. Am. Chem. Soc.* **2000**, *122*, 2124–2125.
 (8) Schatz, M.; Becker, M.; Thaler, F.; Hampel, F.; Shindler, S.; Jacobson, R. R.; Tyeklar, Z.; Murthy, N. N.; Ghosh, P.; Chen, Q.; Zubieta, J.; Karlin, K. D. *Inorg. Chem.* **2001**, *40*, 2312–2322.
 (9) Lin, B. S.; Holm, R. H. *Inorg. Chem.* **1998**, *37*, 4898–4908.
 (10) Zhang, C. X.; Kaderli, S.; Costas, M.; Kim, E.; Neuhold, Y.; Karlin, K. D.; Zuberbühler, A. D. *Inorg. Chem.* **2003**, *42*, 1807–1824.
 (11) Tolman, W. B. *Acc. Chem. Res.* **1997**, *30*, 227–237.
 (12) Zhang, C. X.; Liang, H.; Kim, E.-I.; Shearer, J.; Helton, M. E.; Kim, E.; Kaderli, S.; Incarvito, C. D.; Zuberbühler, A. D.; Rheingold, A. L.; Karli, K. D. *J. Am. Chem. Soc.* **2003**, *125*, 634–635.
 (13) Hu, Z.; Williams, R. D.; Tran, D.; Spiro, T. G.; Gorun, S. M. *J. Am. Chem. Soc.* **2000**, *122*, 3550–3557.
 (14) Taki, M.; Teramae, S.; Nagamoto, S.; Tachi, Y.; Kitagawa, T.; Itoh, S.; Fukuzumi, S. *J. Am. Chem. Soc.* **2002**, *124*, 6367–6397.

- (15) SAINTPLUS Version 6.02, Bruker AXS, Madison, WI, 1999.
 (16) (a) SHELXTL Version 5.1, Bruker AXS, Madison, WI, 1998. (b) Sheldrick, G. M. SHELXL-97, Program for Crystal Structure Refinement, University of Göttingen, Germany, 1997.
 (17) Black, G.; Deep, E.; Corson, B. B. *J. Org. Chem.* **1948**, *13*, 14–21.

Table 1. Crystallographic and Refinement Details for Compounds [Cu(MeDPMA)(MeO)]₂(ClO₄)₂ (**1**), [Cu(MePMPEA)(MeO)]₂(ClO₄)₂ (**2**), [Cu(FDPMA)(OH)]₂(ClO₄)₂·CH₃OH (**3**), [Cu(FPMPEA)(MeO)]₂(ClO₄)₂ (**4**), [Cu(DPMA)(Cl)]₂(ClO₄)₂·0.33 CH₃OH (**5**) and [Cu(BiBzMePMA)(MeO)]₂(ClO₄)₂·2H₂O (**6**)

parameter	Value					
	1	2	3	4	5	6
formula	C ₄₂ H ₄₈ Cl ₂ Cu ₂ N ₆ O ₁₀	C ₄₄ H ₅₂ Cl ₂ Cu ₂ N ₆ O ₁₀	C ₄₁ H ₄₂ Cl ₂ Cu ₂ F ₆ N ₆ O ₁₁	C ₄₄ H ₄₆ Cl ₂ Cu ₂ F ₆ N ₆ O ₁₀	C _{38.33} H _{39.33} Cl ₄ Cu ₂ N ₆ O _{8.33}	C ₄₄ H ₅₄ Cl ₂ Cu ₂ N ₄ O ₁₂
fw	994.8	1022.9	1104.8	1130.8	987.58	1028.43
cryst syst	monoclinic	monoclinic	monoclinic	monoclinic	hexagonal	triclinic
space group	<i>P</i> 2 ₁ / <i>c</i>	<i>P</i> 2 ₁ / <i>c</i>	<i>P</i> 2 ₁ / <i>c</i>	<i>P</i> 2 ₁ / <i>c</i>	<i>R</i> $\bar{3}$	<i>P</i> $\bar{1}$
lattice parameters						
<i>a</i> (Å)	11.740(2)	9.907(5)	16.538(4)	10.097(1)	27.901(2)	10.051(10)
<i>b</i> (Å)	13.587(2)	12.832(6)	13.352(3)	12.894(1)	27.901(2)	10.492(11)
<i>c</i> (Å)	14.656(2)	18.477(9)	21.929(5)	18.439(2)	14.459(1)	12.462(13)
α (°)	90	90	90	90	90	81.857(16)
β (°)	111.431(3)	104.449(9)	97.901(4)	103.570(1)	90	77.019(16)
γ (°)	90	90	90	90	120	75.086(16)
<i>V</i> (Å ³)	2176.1(5)	2274(2)	4797(2)	2333.7(4)	9747(1)	1233(2)
<i>Z</i>	2	2	4	2	9	1
<i>F</i> ₀₀₀	1028	1060	2232	1156	4573	530
<i>D</i> _c (g/cm ³)	1.518	1.494	1.524	1.609	1527	1.381
cryst size (mm ³)	0.50 × 0.50 × 0.20	0.50 × 0.40 × 0.20	0.90 × 0.60 × 0.10	0.80 × 0.50 × 0.10	0.80 × 0.80 × 0.60	0.60 × 0.60 × 0.40
2 θ range (°)	3.72–55.10	3.90–50.02	3.58–56.58	3.90–56.08	3.28–55.18	3.36–50.94
μ (mm ⁻¹)	1.165	1.117	1.084	1.114	1.287	1.032
index ranges	–14 ≤ <i>h</i> ≤ 14, –17 ≤ <i>k</i> ≤ 17, –19 ≤ <i>l</i> ≤ 18	–11 ≤ <i>h</i> ≤ 11, 0 ≤ <i>k</i> ≤ 15, 0 ≤ <i>l</i> ≤ 21	–21 ≤ <i>h</i> ≤ 21, 0 ≤ <i>k</i> ≤ 17, 0 ≤ <i>l</i> ≤ 27	–12 ≤ <i>h</i> ≤ 13, –16 ≤ <i>k</i> ≤ 16, –23 ≤ <i>l</i> ≤ 24	–34 ≤ <i>h</i> ≤ 36, –36 ≤ <i>k</i> ≤ 35, –18 ≤ <i>l</i> ≤ 18	–11 ≤ <i>h</i> ≤ 11, –9 ≤ <i>k</i> ≤ 12, –14 ≤ <i>l</i> ≤ 14
number of reflns						
collected	4799	4002	10907	5235	4904	4092
observed	2829	1064	3845	3980	4039	2758
<i>R</i> ^a	0.0770	0.0535	0.0908	0.0498	0.0412	0.0768
<i>R</i> _w ^b	0.1706	0.0722	0.2159	0.1325	0.1235	0.2020
final difference (e/Å ³)	0.659, –0.579	0.356, –0.253	1.006, –0.660	0.804, –0.465	0.830, –0.302	0.735, –0.628

^a $R = \sum ||F_o| - |F_c|| / \sum |F_o|$. The wavelength of Mo K α radiation used was $\lambda = 0.71073$ Å. ^b $R_w = [\sum w(|F_o| - |F_c|)^2 / \sum w(F_o)^2]^{1/2}$, where $w = 1/\sigma^2(F_o)$. The wavelength of Mo K α radiation used was $\lambda = 0.71073$ Å.

ether portions, and the combined organic phase was dried with anhydrous sodium sulfate. The desiccant was filtered and the solvent evaporated to give 8 g (42%) of product.

(6-Bromomethyl)(2-trifluoromethyl)pyridine. This reagent was obtained by bromination of (2-trifluoromethyl)(6-methyl)pyridine with NBS under experimental conditions similar to those described previously for the methyl analogue.

(2-Pyridylmethyl)(6-methyl-2-pyridylmethyl)amine and **(2-pyridylethyl)(6-methyl-2-pyridylmethyl)amine** were obtained via the reaction of (2-bromomethyl)(6-methyl)pyridine with 2-pyridylmethylamine and 2-pyridylethylamine, respectively, under the same conditions described for the nonsubstituted amines.

(2-Pyridylmethyl)(6-trifluoromethyl-2-pyridylmethyl)amine and **(2-pyridylethyl)(6-trifluoromethyl-2-pyridylmethyl)amine** were obtained in a similar manner, using (6-bromomethyl)(2-trifluoromethyl)pyridine.

Syntheses of Ligands. All the ligands were prepared via reaction of the appropriate secondary amine, with benzyl bromide in CH₃CN as the solvent. A typical procedure is described for DPMA.

Bis-(2-pyridylmethyl)-benzylamine (DPMA). Benzyl bromide (0.05 mol) was added to di-(2-pyridylmethyl)amine (0.05 mol) in 100 cm³ of CH₃CN and excess solid Na₂CO₃, and the reaction mixture was refluxed with stirring for 24 h. The solid was centrifuged and the resulting solution was evaporated. The obtained reddish oil was purified by column chromatography, using chloroform as the eluent. ¹H NMR data (δ /ppm vs Me₄Si) in CDCl₃: 3.68 (s, 2H, Ph-CH₂), 3.81 (s, 4H, Py-CH₂), 7.13–8.51 (several multiplets, 13 H, phenyl and pyridine protons).

(2-Pyridylmethyl)(2-pyridylethyl)-benzylamine (PMPEA). ¹H NMR data (δ /ppm vs Me₄Si) in CDCl₃: 3.0 (4H, dt, CH₂-CH₂), 3.65 (s, 2H, Ph-CH₂), 3.82 (s, 2H, Py-CH₂), 7.1–8.5 (several multiplets, 13 H, phenyl and pyridine protons).

(2-Pyridylmethyl)(6-methyl-2-pyridylmethyl)-benzylamine (MeDPMA). ¹H NMR data (δ /ppm vs Me₄Si) in CDCl₃: 2.52 (3H, s, CH₃), 3.68 (2H, s, Ph-CH₂), 3.78 (2H, s, R-Py-CH₂), 3.81 (2H, s, Py-CH₂), 7.0–8.52 (several multiplets, 12 H, phenyl and pyridine protons).

(2-Pyridylmethyl)(6-trifluoromethyl-2-pyridylmethyl)-benzylamine (FDPMA). ¹H NMR data (δ /ppm vs Me₄Si) in CDCl₃: 3.71 (2H, s, Ph-CH₂), 3.83 (2H, s, Py-CH₂), 3.88 (2H, s, R-Py-CH₂), 7.1–8.53 (several multiplets, 12 H, phenyl and pyridine protons).

(2-Pyridylethyl)(6-methyl-2-pyridylmethyl)-benzylamine (MePMPEA). ¹H NMR data (δ /ppm vs Me₄Si) in CDCl₃: 2.51 (3H, s, CH₃), 2.9 (4H, dt, CH₂-CH₂), 3.61 (2H, s, Ph-CH₂), 3.64 (2H, s, R-Py-CH₂), 7.0–8.5 (several multiplets, 12 H, phenyl and pyridine protons).

(2-Pyridylethyl)(6-trifluoromethyl-2-pyridylmethyl)-benzylamine (FPMPEA). ¹H NMR data (δ /ppm vs Me₄Si) in CDCl₃: 2.9 (4H, dt, CH₂-CH₂), 3.6 (2H, s, Ph-CH₂), 3.8 (2H, s, R-Py-CH₂), 7.1–8.5 (several multiplets, 12 H, phenyl and pyridine protons).

Bis-benzyl-(6-methyl-2-pyridylmethylamine (BiBzMePMA). This ligand was prepared by the same general method, via the reaction of 1 mol of 2-pyridylmethylamine with 2 mol of benzyl bromide. ¹H NMR data (δ /ppm vs Me₄Si) in CDCl₃: 2.5 (3H, s, CH₃), 3.6 (4H, s, Ph-CH₂), 3.7 (2H, s, R-Py-CH₂), 6.95–7.55 (several multiplets, 13 H, phenyl and pyridine protons).

Oxidized Complexes [CuL(OR)]₂(ClO₄)₂. General Procedure. A degassed methanol solution of the appropriate ligand (2 mmol) was added to a suspension of Cu(CH₃CN)₄ClO₄ (2 mmol) in 10 cm³ of MeOH, under nitrogen. The mixture was stirred for 30 min, giving a yellow solution, and then the flask was open to the atmosphere. The solution turns blue or greenish blue and the solid product separates over time. Recrystallization from MeOH gives,

Oxidation of Cu Complexes with Tridentate Ligands

in most cases, crystals suitable for X-ray diffraction (XRD) studies, with the exception of the nonsubstituted ligands. The oxidation products correspond to binuclear copper(II) complexes bridged by two methoxo (or hydroxo in the case of FDPMA) moieties: $[\text{CuL}(\text{OR})_2(\text{ClO}_4)_2]$, where $\text{R} = \text{H}, \text{Me}$, (**1–4, 6**).

Oxidation of the Cu(I) complex with the DPMA ligand, using CH_2Cl_2 as the solvent, instead of MeOH, gives blue crystals of a chloride-containing copper(II) complex: $[\text{Cu}(\text{DPMA})\text{Cl}]_2(\text{ClO}_4)_2 \cdot 0.33 \text{CH}_3\text{OH}$ (**5**).

$[\text{Cu}(\text{MeDPMA})(\text{MeO})_2(\text{ClO}_4)_2]$ (**1**). Anal. Calcd for $\text{C}_{42}\text{H}_{48}\text{N}_6\text{Cl}_2\text{O}_{10}\text{Cu}_2$: C, 50.66; H, 4.86; N, 8.44; Cu, 12.77. Found: C, 51.17; H, 4.80; N, 8.27; Cu, 12.58.

$[\text{Cu}(\text{MePMPEA})(\text{MeO})_2(\text{ClO}_4)_2]$ (**2**). Anal. Calcd for $\text{C}_{44}\text{H}_{52}\text{N}_6\text{Cl}_2\text{O}_{10}\text{Cu}_2$: C, 51.62; H, 5.12; N, 8.21; Cu, 12.42. Found: C, 52.24; H, 5.16; N, 8.13; Cu, 12.28.

$[\text{Cu}(\text{FDPMA})(\text{OH})_2(\text{ClO}_4)_2 \cdot \text{CH}_3\text{OH}]$ (**3**). Anal. Calcd for $\text{C}_{41}\text{H}_{42}\text{F}_6\text{N}_6\text{Cl}_2\text{O}_{11}\text{Cu}_2$: C, 44.45; H, 3.83; N, 7.59; Cu, 18.3. Found: C, 44.01; H, 3.77; N, 7.36; Cu, 11.35.

$[\text{Cu}(\text{FPMPEA})(\text{MeO})_2(\text{ClO}_4)_2]$ (**4**). Anal. Calcd for $\text{C}_{44}\text{H}_{46}\text{F}_6\text{N}_6\text{Cl}_2\text{O}_{10}\text{Cu}_2$: C, 46.69; H, 4.10; N, 7.43; Cu, 12.23. Found: C, 46.93; H, 4.11; N, 7.35; Cu, 11.02.

$[\text{Cu}(\text{DPMA})(\text{Cl})_2(\text{ClO}_4)_2 \cdot 0.33 \text{CH}_3\text{OH}]$ (**5**). Anal. Calcd for $\text{C}_{38.33}\text{H}_{39.66}\text{N}_6\text{Cl}_4\text{O}_{8.33}\text{Cu}_2$: C, 46.66; H, 4.06; N, 8.52; Cu, 12.88. Found: C, 45.95; H, 4.13; N, 8.32; Cu, 12.44.

$[\text{Cu}(\text{BiBzMePMA})(\text{MeO})_2(\text{ClO}_4)_2 \cdot 2\text{H}_2\text{O}]$ (**6**). Anal. Calcd for $\text{C}_{44}\text{H}_{54}\text{N}_4\text{Cl}_2\text{O}_{12}\text{Cu}_2$: C, 51.24; H, 5.29; N, 5.45; Cu, 12.35. Found: C, 52.54; H, 5.12; N, 5.05; Cu, 12.32.

(Caution: Perchlorate complexes are potentially explosive and should be handled with care. However, the small quantities used in our studies were not determined to present a hazard.)

Results and Discussion

Preparations of Ligands. The new ligands were synthesized according to general methods, to prepare amines via the reaction of a secondary amine and an alkyl halide. The necessary secondary amines were made in a similar manner. The noncommercially available halides were synthesized by bromination of the methyl group with *N*-bromo-succinimide (NBS) under UV light.

The trifluoromethyl-substituted pyridine was obtained by fluorination of the carboxylic acid with SF_4 in liquid HF.¹⁸ Other reaction schemes exhibited unsuccessful results.

Syntheses of Copper Complexes. $\text{Cu}(\text{AN})_4\text{ClO}_4$ reacts with a stoichiometric amount of the pyridyl ligands in methanol to give yellow solutions of the copper(I) complexes that were oxygenated at room temperature to give blue or green-blue solutions of the copper(II) products. The spectra of the final resultant mixture show broad bands at 600–700 nm, because of the d–d transitions of the Cu(II) ions. No bands due to LMCT are observed in the 350–400 nm range (alkoxo or hydroxo to Cu(II) bands).

Crystals suitable for XRD were obtained only with the substituted tridentate ligands and the bidentate ligand, by recrystallization in methanol. These copper(II) complexes were characterized by X-ray analysis and magnetic susceptibility.

Compound **5** was obtained by oxidation of the Cu(I) complex with the nonsubstituted DPMA ligand, in dichloro-

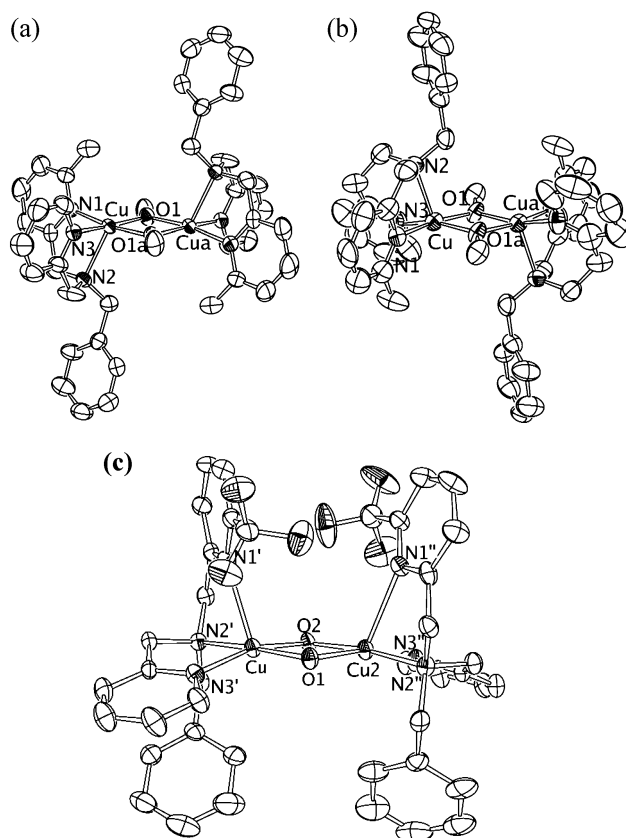


Figure 1. Ortep structure plots for (a) **1**, (b) **2**, and (c) **3**, showing the partial numbering scheme. H atoms, counteranions, and solvent were omitted for clarity. Displacement ellipsoids at 50% probability level.

methane as the solvent. The chloride probably resulted from reaction with the solvent, as has been observed in other related systems.¹⁹

Crystal Structures. Table 1 shows crystallographic and refinement details for compounds **1–6**. Panels a, b, and c in Figure 1 show structural diagrams for **1**, **2**, and **3**, respectively, whereas panels a, b, and c of Figure 2 show structural diagrams for **4**, **5**, and **6**, respectively. Table 2 shows selected bond distances and angles for compounds **1–6**.

Chart 2 shows a diagram of the connectivity within the series **1–6**. For complex **6** ($\text{R} = \text{Me}$), $n = 1$ and the nonsubstituted pyridyl group has been replaced by a non-coordinating phenyl ring. Each compound is formed by two (amine) Cu^{2+} fragments, which are bridged by chloride (**5**), methoxo (**1**, **2**, **4**, and **6**) or hydroxo (**3**) groups in a double μ_2 -fashion. Perchlorate counteranions provide charge balance in all cases. The coordination geometry around each Cu center can be well-described as a square-base pyramid, except for **6**, where the lack of one pyridyl ring leaves each Cu(II) in a square planar environment. For **1**, **2**, and **4**, the amine ligand occupies two of the basal positions through two pyridyl ring N atoms, whereas the aliphatic N atom coordinates the apical one and the bridging ligands occupy the two remaining basal positions. The trifluoromethyl-substituted pyridyl ring, instead of the aliphatic N atom, occupies the apical position in **3**. For **5**, the situation is slightly

(18) Raasch, M. S. *J. Org. Chem.* **1962**, *27*, 1406–1409.

(19) Wei, N.; Murthy, N. N.; Chen, Q.; Zubieta, J.; Karlin, K. D. *Inorg. Chem.* **1994**, *33*, 1953–1965.

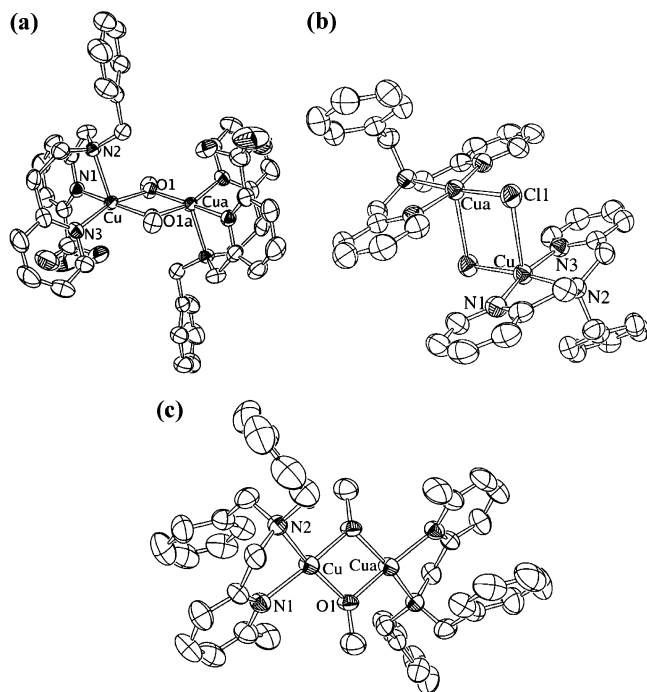
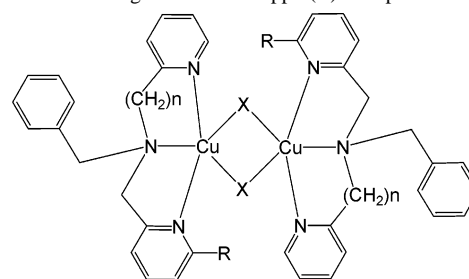


Figure 2. Ortep structure plots for (a) **4**, (b) **5**, and (c) **6**, showing the partial numbering scheme. H atoms, counteranions, and solvent were omitted for clarity. Displacement ellipsoids at 50% probability level.

different, compared to the others complexes: the tripodal amine occupies three basal positions, whereas the bridging chlorides fill the remaining basal and apical ones. This axial–

Chart 2. General Diagram for the Copper(II) Complexes



Compound number	n	R	X
1	1	Me	MeO
2	2	Me	MeO
3	1	CF ₃	OH
4	2	CF ₃	MeO
5	1	H	Cl

equatorial bridging mode is well-known for halide-bridged copper complexes.²⁰

The aliphatic chain between the amino N atom and the aromatic ring imposes some sterical restraints on the ligand to reach ideal square-base pyramid coordination geometry around each Cu center. This is mainly reflected in some deviation of the apical N atom from its ideal position perpendicular to the base position: the angle defined by this plane and the Cu–N(apical) vector is 19.2°, 14.2°, 18.3°, and 14.4° for **1**, **2**, **3**, and **4**, respectively. The values, as expected, are slightly higher when $n = 1$ (**1** and **3**). Despite the distortions, the coordination geometry still can be well-

Table 2. Selected Bond Distances and Angles for [Cu(MeDPMA)(MeO)]₂(ClO₄)₂ (**1**), [Cu(MePMPEA)(MeO)]₂(ClO₄)₂ (**2**), [Cu(FDPMA)(OH)]₂(ClO₄)₂·CH₃OH (**3**), [Cu(FPMPEA)(MeO)]₂(ClO₄)₂ (**4**), [Cu(DPMA)(Cl)]₂(ClO₄)₂·0.33 CH₃OH (**5**), and [Cu(BiBzMePMA)(MeO)]₂(ClO₄)₂·2H₂O (**6**)

1		2		3		4		5		6	
Bond Distances (Å)											
Cu–O1	1.919(4)	Cu–O1	1.930(4)	Cu1–O1	1.923(5)	Cu–O1	1.949(2)	Cu–N1	1.979(2)	Cu–O1	1.913(4)
Cu–O1 ^a	1.931(4)	Cu–O1 ^b	1.941(4)	Cu2–O1	1.934(5)	Cu–O1 ^b	1.943(2)	Cu–N2	2.031(2)	Cu–O1 ^d	1.921(4)
Cu–N1	1.992(5)	Cu–N1	2.001(6)	Cu1–O2	1.931(5)	Cu–N1	2.082(3)	Cu–N3	1.990(2)	Cu–N1	2.008(5)
Cu–N2	2.307(4)	Cu–N2	2.227(6)	Cu2–O2	1.913(5)	Cu–N2	2.253(2)	Cu–Cu ^c	3.566(1)	Cu–N2	2.038(4)
Cu–N3	2.012(5)	Cu–N3	2.010(7)	Cu1–N1′	2.422(7)	Cu–N3	2.003(3)	Cu–Cl1	2.2490(7)	Cu–Cu ^d	2.967(3)
Cu–Cu ^a	3.022(1)	Cu–Cu ^b	3.049(2)	Cu1–N2′	2.025(6)	Cu–Cu ^b	3.0506(7)	Cu–Cl1 ^c	2.892(1)		
				Cu1–N3′	1.976(6)						
				Cu2–N1′′	2.422(7)						
				Cu2–N2′′	2.033(6)						
				Cu2–N3′′	1.984(7)						
				Cu1–Cu2	2.960(1)						
Bond Angles (deg)											
O1–Cu–O1 ^a	76.6(2)	O1–Cu–O1 ^b	76.1(2)	O1–Cu1–O2	79.3(2)	O1–Cu–O1 ^b	76.8(1)	N1–Cu–N2	83.12(8)	O1–Cu–O1 ^d	78.6(2)
O1–Cu–N1	170.1(2)	O1–Cu–N1	167.8(2)	O1–Cu1–N1′	109.6(2)	O1–Cu–N1	167.6(1)	N1–Cu–N3	165.7(1)	O1–Cu–N1	100.7(2)
O1–Cu–N2	107.5(2)	O1–Cu–N2	105.4(2)	O1–Cu1–N2′	175.0(2)	O1–Cu–N2	107.5(1)	N2–Cu–N3	82.6(1)	O1–Cu–N2	160.9(2)
O1–Cu–N3	95.3(2)	O1–Cu–N3	95.2(3)	O1–Cu1–N3′	98.8(3)	O1–Cu–N3	94.2(1)	N1–Cu–Cl1	97.51(6)	N1–Cu–N2	84.0(2)
N1–Cu–N2	81.1(2)	N1–Cu–N3	95.7(3)	O2–Cu1–N1′	100.3(2)	N1–Cu–N3	95.3(1)	N2–Cu–Cl1	174.47(6)	Cu–O1–Cu ^d	101.4(2)
N2–Cu–N3	79.2(2)	N2–Cu–N3	92.6(3)	O2–Cu1–N2′	97.0(2)	N2–Cu–N3	94.6(1)	N3–Cu–Cl1	96.71(7)		
Cu–O1–Cu ^a	103.4(2)	Cu–O1–Cu ^b	103.9(2)	O2–Cu1–N3′	163.3(2)	Cu–O1–Cu ^b	103.2(1)	N1–Cl1 ^c –Cu	90.00(6)		
				O1–Cu2–N1′′	99.9(2)			N2–Cl1 ^c –Cu	90.90(7)		
				O1–Cu2–N2′′	96.4(2)			N3–Cl1 ^c –Cu	92.37(6)		
				O1–Cu2–N3′′	164.7(3)			Cu–Cl1–Cu ^c	86.87(6)		
				O2–Cu2–N1′′	112.5(2)						
				O2–Cu2–N2′′	172.1(2)						
				O2–Cu2–N3′′	98.9(3)						
				N2′–Cu1–N3′	83.8(3)						
				N2′′–Cu2–N3′′	83.2(3)						
				Cu1–O1–Cu2	100.3(2)						
				Cu2–O2–Cu1	100.7(2)						

^a $-x, -y + 1, -z$. ^b $-x + 1, -y + 2, -z + 1$. ^c $-y + 1, x - y + 1, z$. ^d $-x + 1, -y + 1, -z + 1$.

described as base square pyramid in all cases, which is confirmed by the τ values (0.0316, 0.0103, 0.1645, 0.0946, and 0.0125 for **1**, **2**, **3**, **4**, and **5**, respectively). This deviation is 0.8° for **5**, where a Cl atom occupies the apical position.

As mentioned previously, the pyramidal or square planar (amine) Cu^{2+} units are connected through bridging ligands to define the dimer complexes. In the case of **1–4** and **6**, there are two μ_2 -hydroxy or alkoxy bridging ligands, which are located in basal positions, whereas the chloride-bridging ligands in **5** occupy axial–equatorial positions. The basal coordination planes of the two Cu centers are coplanar for **1**, **2**, **4**, and **6** (forced by the presence of a symmetry center between the metal atoms), whereas, in **3**, they define a dihedral angle of $12.2(6)^\circ$. The apical bridging in **5** leaves the neighboring basal planes parallel and separated by $2.892(1) \text{ \AA}$, which is the Cu–Cl long bond distance. This bridging mode is reflected on a longer Cu–Cu distance ($3.566(1) \text{ \AA}$), when compared to **1–4** and **6**, which range from $2.960(1) \text{ \AA}$ in **3** to $3.051(1) \text{ \AA}$ in **4**. Following the tendency of the Cu–Cu distance, the bridging angle (Cu–O–Cu) has its minimum values for complex **3** (100.3° and 100.7°), whereas the values for **1**, **2**, and **4** are $103.4(2)^\circ$, $103.9(2)^\circ$, and $103.2(2)^\circ$, respectively, which suggests that, for this last series of compounds, the length of the chain alkyl linker or the substituent R does not strongly determine this value. The value for the Cu–O–Cu angle in a related bis- μ -hydroxo copper complex with the tridentate ligand bis-(2-pyridylethyl)benzylamine was reported to be $101.0(2)^\circ$ and the Cu–Cu distance is 3.271 \AA , compared to a value of $\sim 3 \text{ \AA}$ in **3**. This difference could result from the different bridging mode of the OH group: equatorial–equatorial in **3** and axial–equatorial in the reported one.²¹

For all the methoxo-bridged compounds, the methyl groups are located on opposite sides of the central Cu_2O_2 plane. The angle defined by this plane and the O–C vectors are 7.51° , 10.88° , 16.96° , and 25.57° for **1**, **2**, **4**, and **6**, respectively. Surprisingly, the higher deviation correspond to **6**, which is a copper dimer without a pyridyl ligand at the apical position, instead of the complex with the sterically demanding trifluoromethyl group.

Considering the sterical repulsion of the bulky pyridyl rings of the (amine) Cu^{2+} units, one may expect them to lie on different sides of the coordinated basal planes, in a trans arrangement, especially if one of the pyridyl rings is substituted ($\text{R} \neq \text{H}$). That is the case for compounds **1**, **2**, and **4**, where apical pyridyl rings lie on opposite sides of the basal coordinated plane. Surprisingly, **3** (with two $\text{R} = \text{CF}_3$ units) shows a cis arrangement. This phenomenon can probably be related to the presence of less sterically demanding hydroxyl groups that serve as the bridging groups in this compound. Interestingly, one of the F atoms on the trifluoromethyl R group points directly to the adjacent pyridyl ring (see Figure 1c).

As the only hydroxyl compound in the series, **3** is the only complex that shows a hydrogen-bonded packing diagram.

Although the hydroxo H atoms were not located by the Fourier difference synthesis, two O atoms of each perchlorate counteranion point directly to the hydroxo O bridging atoms, at 3.564 and 3.067 \AA , from O1 and O2, respectively, which suggests hydrogen bonding. The two perchlorate anions from consecutive dimeric units (x, y, z and $x, y - 1, z$) are separated in this way by 5.147 \AA , and the corresponding Cu centers are separated by $\sim 12 \text{ \AA}$.

Magnetic Properties. The alkoxy-bridged complexes **1**, **2**, **4**, and **6** were measured at room temperature and are electroparamagnetic resonance (EPR) silent. Variable-temperature magnetic susceptibility measurements were performed in the $10\text{--}300 \text{ K}$ temperature range on all the reported compounds.

The bis-methoxo bridged complexes (**1**, **2**, **4**, and **6**) show no maximum in the molar magnetic susceptibility within the studied temperature range; only an increase in the susceptibility toward values greater than room temperature is observed. Figure 3 shows the variation of the susceptibility with temperature for the complex with MeDPMA (**1**).

This magnetic behavior is representative of the entire family of compounds (complexes **1**, **2**, **4**, and **6**). The increase in magnetic susceptibility at higher temperatures ($>350 \text{ K}$) suggests that a strong antiferromagnetic interchange operates between the Cu atoms in these complexes. It is generally accepted that the magnitude of the $2J$ parameter (which is an indicator of the magnetic interaction between the Cu centers), in alkoxy-bridged and analogous phenoxo- or hydroxo-bridged copper(II) compounds, is mainly related to the Cu–O–Cu angle.^{22–24} A linear relationship between $2J$ and the bridging angle has been proposed for these compounds. The Cu–O–Cu angle, in our pentacoordinated bis- μ -methoxo-bridged complexes, varies from $103.2(1)^\circ$ to $103.9(2)^\circ$. The $-2J$ values are expected to be $>400 \text{ cm}^{-1}$ and no maximum within the measured temperature range should be observed, in accordance with the measured behavior. A fit of the experimental data to the Bleaney–Bowers equation²⁵ (see below) gives values of $-2J = 1280 \text{ cm}^{-1}$, $g = 2.0$, and $\rho = 0.01$ (see Figure 3).

Figure 4 shows a plot of the susceptibility versus temperature data for the bis- μ -hydroxo-bridged complex obtained with FDPMA (**3**). The curve is typical of antiferromagnetically coupled pairs of Cu^{2+} ions and was fitted to the Bleaney–Bowers equation²⁵ for copper dimers:

$$\chi_M = \frac{2N\beta^2 g^2}{3k(T - \Theta)} \left[1 + \frac{1}{3} \exp\left(-\frac{2J}{kT}\right) \right]^{-1} (1 - \rho) + \frac{(N\beta^2 g^2)\rho}{4kT} + N\alpha \quad (1)$$

using the isotropic (Heisenberg) exchange Hamiltonian ($H = -2JS_1 \cdot S_2$), where χ_M is the magnetic susceptibility (expressed per mole of dimer), Θ is a corrective term for interdimer interactions,²⁶ and all the other parameters have

(20) Hatfield, W. E. *Inorg. Chem.* **1981**, *22*, 833–837.

(21) Karlin, K. D.; Gultneh, Y.; Hayes, J.; Zubieta, J. *Inorg. Chem.* **1984**, *23*, 519–521.

(22) Handa, M.; Koga, N.; Kida, S. *Bull. Chem. Soc. Jpn.* **1988**, *61*, 3853–3857.

(23) Thompson, L. K.; Mandal, S. K.; Tandon, S. J.; Budson, J. N.; Park, M. K. *Inorg. Chem.* **1996**, *35*, 3117–3125.

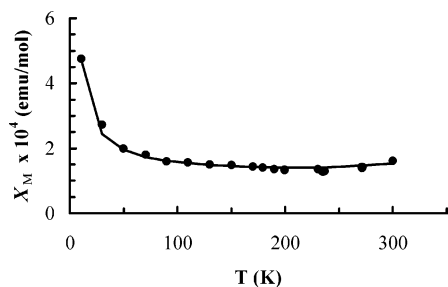


Figure 3. Magnetic data for $[\text{Cu}_2(\text{MeDPMA})(\text{MeO})_2](\text{ClO}_4)_2$ (**1**). Solid line was calculated from eq 1.

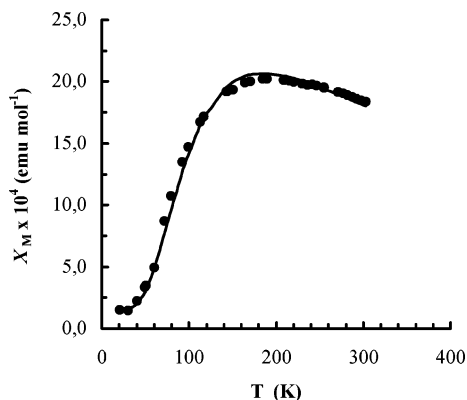


Figure 4. Magnetic data for $[\text{Cu}_2(\text{FDPMA})(\text{OH})_2](\text{ClO}_4)_2 \cdot \text{MeOH}$ (**3**). Solid line was calculated from eq 1.

their usual meanings. The best data fit gives $-2J = 195 \text{ cm}^{-1}$, $\Theta = -20 \text{ K}$, and $\rho = 0.003$. The value for the $-2J$ parameter is in the range expected for a bis- μ -hydroxo bridged copper(II) complex with a Cu–O–Cu angle of ca. 100° , as expected from the dependence of $2J$ on the bond angle that has been proposed for these types of complexes.²⁴

The X-ray structure of this complex shows an intermolecular hydrogen-bonding pattern of the bridging hydroxyl groups through the perchlorate anions that may account for the observed Θ value.

The magnetic behavior of the chloride-bridged complex **5** is shown in Figure 5. The best fit obtained with eq 1 gives $2J = 21 \text{ cm}^{-1}$, $g = 2.09$, and $\rho = 0.004$. The $2J$ value indicates a ferromagnetic interaction between the copper centers. The dependence of $\chi_M T$ versus T agrees with this ferromagnetic coupling. This is a result of the bridging mode: one Cl atom that occupies a basal coordination site in one Cu atom occupies an apical position in the coordination sphere of the second Cu atom.

Conclusion

Karlin and co-workers^{12,27} and other researchers¹⁴ have demonstrated that simple mononuclear copper(I) complexes with bidentate, tridentate, and tetradentate ligands are useful

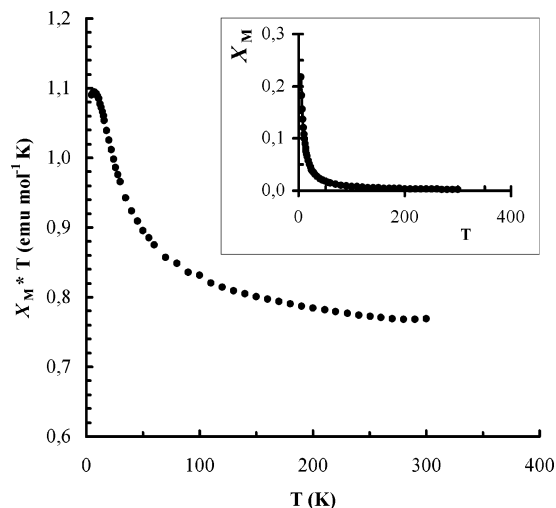


Figure 5. Plot of $\chi_M T$ versus temperature (T) data for $[\text{Cu}_2(\text{DPMA})(\text{Cl})_2](\text{ClO}_4)_2 \cdot 0.33 \text{ MeOH}$ (**5**). Inset shows the dependence of the magnetic susceptibility with T ; the solid line was calculated from eq 1.

precursors of binuclear copper–dioxygen (Cu_2O_2) adducts. Ligand electronics and steric effects greatly influence the type, ease of formation, and subsequent reactivity of dioxygen adducts. Many ligands have been used to study the Cu/O₂ chemistry, for the purpose of tuning their reactivity. In this work, we have synthesized new bidentate and tridentate pyridyl ligands. The binuclear copper(II) complexes, resulting from the oxidation of the corresponding copper(I) complexes, have been characterized by X-ray diffraction and magnetic studies. The binuclear copper(II) complexes are bridged by methoxo-, hydroxo-, or chloride groups. Magnetic susceptibility data show that, in the methoxo-bridged complexes, a strong antiferromagnetic coupling operates between the Cu centers, whereas the hydroxo complex shows a moderated antiferromagnetic interchange and the Cl one is ferromagnetic. Preliminary studies show that the copper(I) complexes are reactive toward oxygen and act as active catalysts for the aerial oxidation of 3,5-diterbutylcatechol. Further studies on the reactivity of these complexes are currently in progress.

Acknowledgment. Financial support from Project FONDECYT 1020101 is gratefully acknowledged. Fundación Andes is greatly acknowledged for the partial financing of the purchase of the Bruker X-ray diffractometer. D.R. acknowledges CONICYT for a doctoral scholarship. D.V. acknowledges a postdoctoral position at CIMAT, financed by Project FONDAP 11980002.

Supporting Information Available: Crystallographic data for compounds **1–6**, in CIF format. This material is available free of charge via the Internet at <http://pubs.acs.org>.

IC049648T

(24) Crawford, V. H.; Richardson, H. W.; Wasson, J. R.; Hodgson, D. J.; Hatfield, W. E. *Inorg. Chem.* **1976**, *15*, 2107.

(25) Bleaney, B.; Bowers, K. D. *Proc. R. Soc. London* **1952**, *A214*, 451.

(26) Sikorov, S.; Bkouche-Waksman, I.; Kahn, O. *Inorg. Chem.* **1984**, *23*, 490.

(27) Sanyal, I.; Mahroof-Tahir, M.; Nasir, M. S.; Ghosh, P.; Cohen, B. I.; Gultneh, Y.; Cruse, R. W.; Farooq, A.; Karlin, K. D.; Liu, S.; Zubieta, J. *Inorg. Chem.* **1999**, *31*, 4322–4332.